Sensors & Transducers Journal, Vol. 105, Issue 6, June 2009, pp. 81-93

www.sensorsportal.com

Sensors & Transducers

ISSN 1726-5479

http://www.sensorsportal.com

Modeling and Analysis of a Bimorph PZT Cantilever Beam Based Micropower Generator

[1]Jyoti AJITSARIA, [1]Song-Yul CHOE, [2]Phil OZMUN, [3]Dongna SHEN and [3]Dong-Joo KIM

[1]Department of Mechanical Engineering, Auburn University, Auburn, Alabama, 36849, USA
[2]Department of Electrical Engineering, Auburn University, Auburn, Alabama, 36849, USA
[3]Materials Research and Education Center, Auburn University, Auburn, Alabama, 36849, USA
E-mail: ajitsjk@auburn.edu

Received: 7 May 2009 /Accepted: 22 June 2009 /Published: 30 June 2009

Abstract: Recent developments in miniaturized sensors, digital processors and wireless communication systems have many desirable applications. The realization of these applications however, is limited by the lack of a similarly sized power source. One method of power harvesting is the use of piezoelectric materials (PZT), which form transducers that are able to interchange electrical energy and mechanical vibration. Many proposed power generation systems employ a piezoelectric component to convert the mechanical energy to electrical energy. In this paper, a formulation of mathematical model is developed that predicts the power conversion for a device that contains a piezoelectric component. Analysis is also done with AC/DC power conversion using a bridge rectifier circuit. Finally, the verification of the models is performed experimentally and comparison has been made with the simulation results. The comparison of simulation results coincide with experimental data quite well. *Copyright © 2009 IFSA.*

Keywords: PZT bimorph, PZT cantilever modeling, PZT generator

1. Introduction

The idea of building portable electronic devices has intrigued researchers in the field of power harvesting. These devices or wireless sensors rely on power supplies with a limited lifespan and has instigated a sharp increase in research of power harvesting. One method of power harvesting is the use of piezoelectric materials (PZT), which form transducers that are able to interchange electrical energy

and mechanical strain or force. Therefore, these materials have been employed as media to transform ambient motion (usually vibration) into electrical energy that can be stored and used as a power source for electronic devices.

Integration of power harvesting devices into sensor suites may allow for free maintenance in comparison with the use of battery which commonly requires a periodic replacement. In addition, potential applications are sensor suites that are physically embedded in an environment and are not accessible for a replacement. Moreover, the physical properties to be measured in the environment vary either relatively slow or do not need to be processed continuously for a high hierarchical system. Consequently, these sensor systems can be effectively operated by intermittent transmission of data gathered and the associated power consumption can be reduced.

The concepts to generate electrical power include devices which harvest energy from the environment. Piezoelectric materials are increasingly employed in these types of micro power generation that converts mechanical energy into electrical energy. The energy harvesting in principle uses strains in the material, which lends themselves to devices that are operated by bending or flexing. The use of the materials yields significant advantages for the power systems. The energy density achievable with piezoelectric devices is potentially greater than that possible with electrostatic or electromagnetic devices [1].

In this research, the ability of piezoelectric materials for energy conversion has been exploited in an application closely related to power generation, the piezoelectric transformer.

The use of the piezoelectric effect to convert mechanical to electrical work in power supply devices has been investigated by many authors. Umeda, et al [2] were among the pioneers to study the PZT generator and proposed an electrical equivalent model being converted from mechanical lumped models of a mass, a spring, and a damper that describe a transformation of the mechanical impact energy into electrical energy in the PZT material. Hausler and Stein [3] proposed a power supply, based on the piezoelectric polymer PVDF, that could be surgically implanted in an animal to convert mechanical work done by an animal during breathing into electrical power. Schmidt [4] investigated harvesting electrical power from the wind by mounting piezoelectric polymers in windmills. Kymisis et al. [5] developed a harvesting energy from ambulatory motion by placing piezoelectric patches in the heels and soles of boots.

Vibrating structures such as composite piezoelectric cantilever beams have been analyzed for their potential to generate electric power from environmental vibrations by Kasyap et al. [6]. Ramsay and Clark [7] considered effects of transverse force on the PZT generator in addition to the force applied in the poling direction. Gonzalez et al [8] analyzed the prospect of the PZT based energy conversion, and suggested several issues to raise the electrical output power of the existing prototypes to the level being theoretically obtained. Smits and Chio [9] studied the electromechanical characteristics of a heterogeneous piezoelectric bender subject to various electrical and mechanical boundary conditions based on internal energy conservation. However, the model used does not provide any formulation for the voltage generation. Other authors such as Huang et al. [10] and DeVoe et al. [11] did the displacement and tip-deflection analysis along the beam and made a comparison with the experimental results. However, both proposals were limited to the actuator mode.

Hwang and Park [12] introduced a new model based on static responses of a piezoelectric bimorph beam in a piezoelectric plate element. Roundy et al. [1, 13, 14] presented a slightly different approach based on the electrical equivalent circuit to describe the PZT bender, which leads to fair matches with the experimental results. However, the analysis only considered a low-g (1-10 m/s2) vibration condition and lacks mechanical dynamics of the structure. Other authors, Lu et al. [15], improved the electrical model by adding an electro-mechanical coupling that represents dynamic behavior of the

beam vibrating under a single degree of freedom. Eggborn [16] developed the analytical models to predict the power harvesting from a cantilever beam and a plate using Bernoulli-beam theory and made a comparison with the experimental result. Kim [17] analyzed the unimorph and bimorph diaphragm structure for the power generation using energy generation and piezoelectric constitutive equations. However, this study was limited to only diaphragm structures that were optimized through numerical analysis and FEM simulation at higher acceleration conditions. Shen et al. [18] investigated the parameters influencing the output energy of a piezoelectric bimorph cantilever beam with a proof mass, where the resonant frequency and robustness of a cantilever structure were considered for enhancing power conversion efficiency and implementing devices at high acceleration conditions.

The studies above had some success in modeling the PZT cantilever beam for voltage and power generation. However many issues such as extensive theoretical analysis of bimorph piezoelectric power generator based on cantilever beam structure with proof mass attached at the end have not been addressed fully. In particular, the efficiency of mechanical to electrical energy conversion is a fundamental parameter for the development and optimization of a power generation device. However, few investigators report a measured and quantified efficiency for their device. Most provide measurements of output power or voltage. In this section, special emphasis has been given to the analytical modeling of efficiency conversion of the bimorph PZT bender with a proof mass in the generator mode. The mathematical models developed are implemented in Matlab/Simulink and experimental verification has been done to assess the accuracy of the various models.

2. Mathematical Model

A lumped parameter model is used to describe the PZT generator. Fig. 1 shows the mechanical model of the system. The equivalent mass, *m*, and spring stiffness, *k*, is determined using a Raleigh-Ritz method with a shape function generated using standard beam theory with a constant acceleration load. The mechanical damping coefficient can be approximated using half amplitude method. F_e is the lumped electrical force generated by electrically induced strains in the piezoelectric layers.

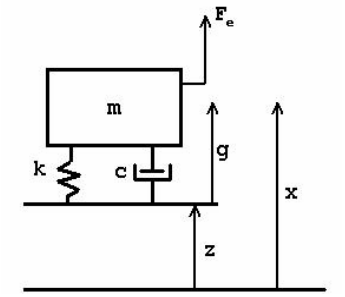

Fig. 1. Lumped mechanical model for PZT generator.

The equation of motion for the generator is essentially that of an accelerometer with an additional force term.

$$\ddot{g}+\frac{c}{m}\dot{g}+\frac{k}{m}g=\frac{F_e}{m}-\ddot{z} \tag{1}$$

The input energy into the system is determined by the force and velocity at the base of the structure. The input force is determined by summing the forces on the system.

$$F_{in} = F_e - c\dot{g} - kg \tag{2}$$

By integrating the force-velocity product the input energy can be evaluated:

$$E_{in}(t) = \int_t F_{in}(\tau)\, z(\dot{\tau})\, d\tau \tag{3}$$

Other energy terms associated with the mechanical system are the energy dissipated by the damper [19]:

$$E_{damp}(t) = \int_t c\, g(\dot{\tau})^2\, d\tau \tag{4}$$

The energy in the spring:

$$E_k(t) = \frac{1}{2} kg(t)^2 \tag{5}$$

The energy in the mass:

$$E_m(t) = \frac{1}{2} m\, x(\dot{t})^2 \tag{6}$$

The last energy term in the mechanical system is the energy transferred to the electrical domain of the generator:

$$E_{me}(t) = \int_t F_e(\tau)\, g(\dot{\tau})\, d\tau \tag{7}$$

While the net flow of energy is from the mechanical to the electrical domain, there can be time intervals where this term is negative.

2.1. Electrical Energy Terms

The lumped electrical model for the PZT generator is shown in Fig. 2.

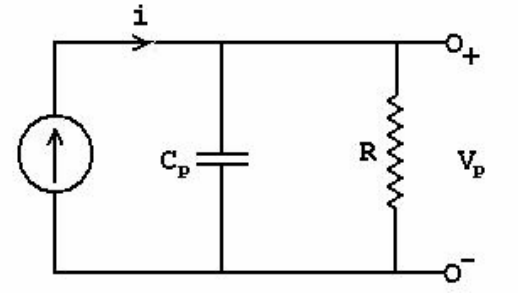

Fig. 2. Lumped electrical model for PZT generator.

This model is more natural than a voltage source model in estimating the voltage-load relationship in cases of an open or shorted load. The voltage dynamic for the electrical subsystem is given:

$$\dot{V}_p + \frac{V_p}{RC_p} = \frac{i}{C_p} \tag{8}$$

The input energy into the electrical circuit is given by the current-voltage relationship:

$$E_{Ein}(t) = \int_t i(\tau) V_p(\tau) d\tau \tag{9}$$

The power (energy) flowing into the electrical circuit is dissipated into the load resistance (output energy), stored in the capacitor, or dissipated as heat. The energy in the capacitor is:

$$E_{cap}(t) = \frac{1}{2} C_p V_p(t)^2 \tag{10}$$

,

where C_p is the complex valued capacitance that incorporates the loss tangent in order to account for dielectric losses that are dissipated as heat. The output energy of the system is:

$$E_{out}(t) = \int_t \frac{V_p(\tau)^2}{R} d\tau \tag{11}$$

And the device efficiency is defined:

$$\eta(t) = \frac{E_{out}(t)}{E_{in}(t)} \tag{12}$$

2.2. Electro-Mechanical Coupling

In order to determine how the electrical and mechanical subsystems are coupled, the displacement-voltage relationship needs to be determined. This can be accomplished by looking at the moment distribution across a section of the beam [20].

$$M = \sum_i \int_{A_i} E_i \left(\frac{y}{R} + d_{31_i} E_i \right) dA_i \tag{13}$$

,

where i denote the sections of the beam, y is the distance from the beams neutral axis, E is Young's Modulus, R is the radius of curvature at the given cross section, d_{31} is the piezoelectric constant, and E is the electric field. In the device being analyzed the beam has 3 layers, a mechanical layer sandwiched between two piezoelectric layers with opposite poling. Rewriting the first equation:

$$M = w \int_{\frac{-t_m}{2}}^{\frac{t_m}{2}} y E_m \frac{y}{R} dy + 2w \int_{\frac{t_m}{2}}^{\frac{t_m}{2}+t_p} y E_p \left(\frac{y}{R} + d_{31} E \right) dy \tag{14}$$

,

where w is the width of the beam, t is the layer thickness (subscripts denoting (p)iezoelectric and (m)echanical layers), and the electric field for the series poling is $\boldsymbol{E}=-V_p/2t_p$. In accordance with typical linear beam theory the radius of curvature is roughly:

$$R = \left(\frac{\partial^2 g}{\partial^2 s} \right)^{-1}, \tag{15}$$

where $g(s)$ is the beam deflection function over the length coordinate of the beam, s. For consistency it should be noted that $g(l)=g$ the gap given in the mechanical model, l being the length of the cantilever. The moment equation for the beam assuming a simple tip load is:

$$M(s) = F(l - s)$$

Combining the previous three equations and integrating two times with respect to s, the tip load, F, can be evaluated:

$$F(g) = \frac{gwE_m {t_m}^3}{4l^3} + \frac{gwE_p}{l^3}\left[\frac{3}{2}{t_m}^2 t_p + 3t_s {t_p}^2 + \frac{1}{2}{t_p}^3\right] + \frac{3wE_p d_{31} E}{2l}\left[t_m t_p + {t_p}^2\right] \tag{16}$$

The terms including g are equivalent to the spring force, kg, from standard beam theory already accounted for in the mechanical model. F_e is the remaining term.

$$F_e(t) = \frac{-3wE_p d_{31} V_p(t)}{4l}\left[t_m + t_p\right] \tag{17}$$

Finally the input current to the electrical circuit can be determined using energy conversion between the two domains.

$$\int_t i(\tau) V_p(\tau) d\tau = -\int_t F_e(\tau)\, \dot{g}(\tau)\, d\tau \tag{18}$$

Solving for i:

$$i(t) = \frac{-3wE_p d_{31}}{4l}\left[t_m + t_p\right]\dot{g}(t) \tag{19}$$

2.3. State Space Analysis

Using the ideas developed above a state-space model of the PZT generator can be developed. The state-space model is given:

$$\begin{bmatrix} \dot{x}_1 \\ \dot{x}_2 \\ \dot{x}_3 \end{bmatrix} = \begin{bmatrix} 0 & 1 & 0 \\ -k/m & -c/m & \alpha/m \\ 0 & -\alpha/C_p & 1/RC_p \end{bmatrix} \begin{bmatrix} x_1 \\ x_2 \\ x_3 \end{bmatrix} + \begin{bmatrix} 0 \\ -a \\ 0 \end{bmatrix} \ddot{z}, \tag{20}$$

where the states are the displacement, velocity, and voltage respectively. The mass, spring constant, damping coefficient, load resistance, and piezoelectric capacitance are the same as discussed previously. The acceleration, a, is the input amplitude in m/s^2. The piezoelectric capacitance, C_p, and the coupling constant, α_p, depend on the poling of the PZT layers.

For poling in the same direction, the wiring is done in parallel:

$$\alpha_p = \frac{3wE_p d_{31}}{2l}\left[t_m + t_p\right] \tag{21}$$

$$C_{p_p} = \frac{2\varepsilon A}{t_p}\left[1 - i\tan\delta\right] \tag{22}$$

3. Experimental Setup

The bimorph PZT bender with an attached proof mass made from Tungsten was constructed as shown in Fig. 3. The bender was composed of a brass center shim sandwiched by two layer of PZT-5H. The thickness of the brass plate and the PZT is 0.134 mm and 0.132 mm, respectively. The length of the bender is 25 mm and width is 3.2 mm. The dimensions of proof mass are length 3.03 mm, width 2.95 mm and height 2.9 mm and the mass is 0.502 grams. In order to investigate parameters of the prototype structure, a test setup was built to excite the bender with a predetermined resonant frequency using a shaker connected via a function generator through amplifier. The system described here is designed to utilize the z-axis vibration as the only vibration source for the device. The characterization of the fabricated cantilever device, the voltage generated was evaluated by connecting a resistor. Fig. 4 illustrates the schematic of experimental setup and a photo for a real setup.

The beam was excited by a sinusoidal input and the steady state voltage was measured across several different resistors. The accuracy of the model was compared against experimental results to demonstrate the ability of the model to accurately predict the amount of power produced by the PZT generator when subjected to transverse vibration. To ensure the model and experimental tests were subjected to the same excitation force an accelerometer was used to calculate the amplitude of the sinusoidal acceleration applied to the beam.

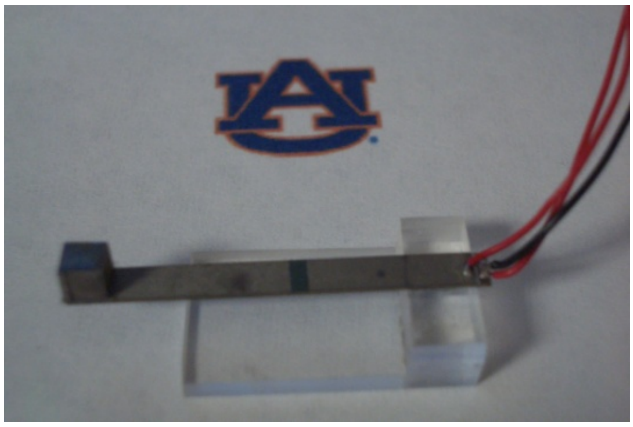

Fig. 3. Bimorph PZT bender.

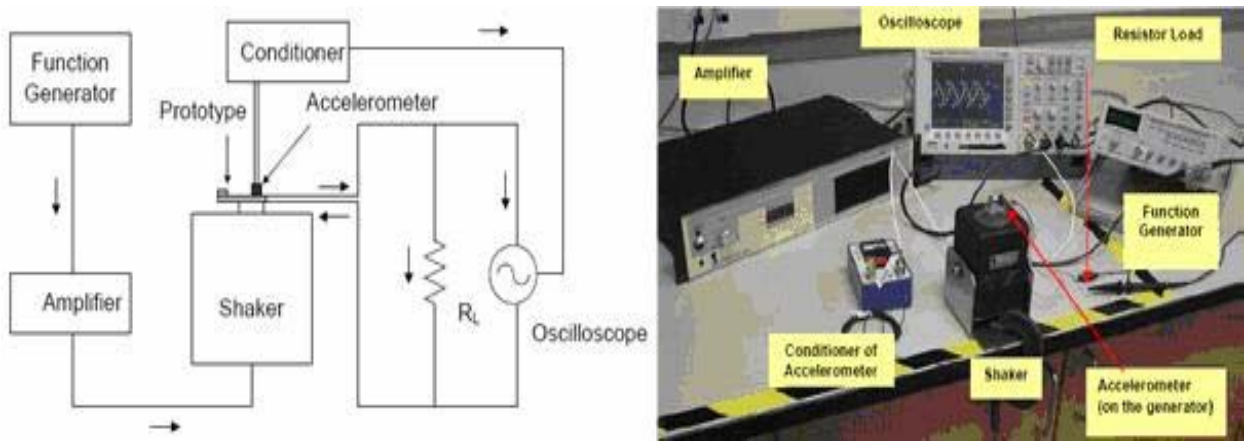

Fig. 4. Schematic and picture of experimental setup.

4. Results and Discussions

4.1. Open Circuit

The accuracy of the model was compared with respect to the time response at an acceleration of the device and the current-voltage characterization as well as the generated power at different resistive load. Experimental data was available for the device being modeled. That data included a device natural frequency of 95 Hz and power and voltage data for different load resistances. The Raleigh-Ritz method used to determine the lumped parameters provided mass and spring coefficients of; m=0.502 grams and k=289.02 N/m (f_o=94 Hz). The damping coefficient was assumed to be; c=0.02 kg/s for all cases.

Fig. 5 shows the comparison of experimental vs. simulation results for open circuit voltage output from the PZT micropower generator. It can be seen from the Fig. 5, that the experimental open circuit output voltage coincides pretty good with the simulation results. The experimental resonant frequency for the structure is 95 Hz, while the simulation resonant frequency is 94 Hz. The maximum experimental voltage was ~22 V (peak to peak) at ~95 Hz, which matches the state-space model well, where the maximum voltage (open loop) was ~23 V (peak-peak), at ~94 Hz.

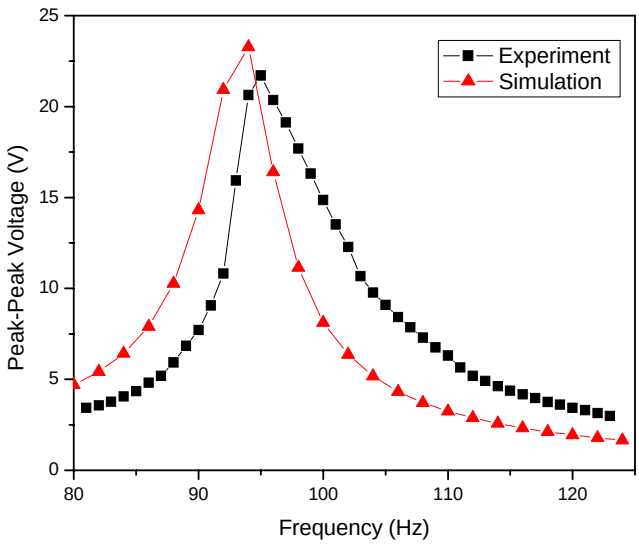

Fig. 5. Comparison of experimental vs. simulation results for frequency vs. voltage output.

4.2. Resistive Load

Fig. 6 shows the trend in output voltage and active power for the PZT micropower generator at resonant frequency with different load resistance, which also coincides with the simulation data pretty well. Although there is slight discrepancy in the optimal load resistance for the experimental and simulation results, for the model, the load and frequency at max power was ~70 kΩ at ~94 Hz while the experimental data has load and frequency at max power of ~80 kΩ at ~95 Hz.

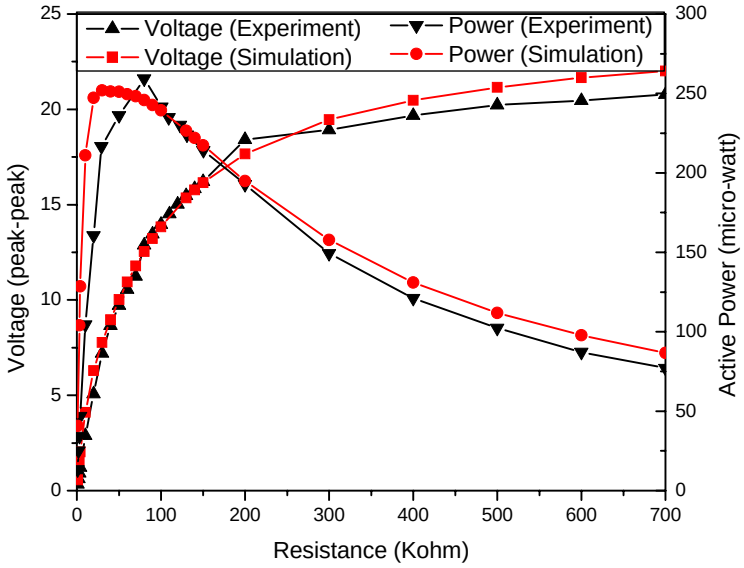

Fig. 6. Comparison of experimental vs. simulation results for voltage vs. load resistance.

Fig. 7 shows the I-V characteristics of the PZT micropower generator. The maximum voltage was ~22 V (peak to peak), the maximum power was ~250 μW. This matches the state-space model well, where the maximum voltage (open loop) was ~23 V (peak), and the maximum power was ~240 μW.

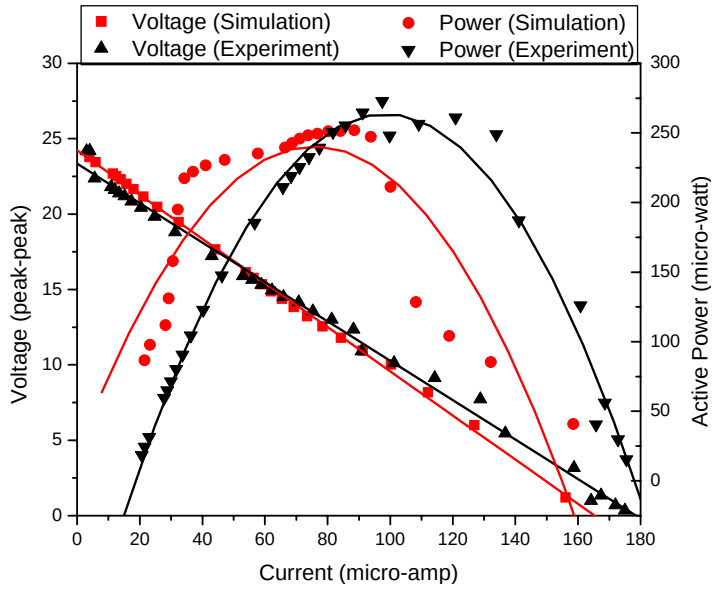

Fig. 7. Comparison of experimental vs. simulation Experimental I-V characteristics.

4.3. Rectifier with Resistive Load

The PZT bender produces an alternating current, whose amplitude varies according to the amplitude of the acceleration and the frequency of vibration. On the other hand, electronic loads connected at the output require a DC voltage with relatively low amplitude. The AC/DC rectifier in the first stage converts the varying AC output voltage delivered by the PZT bender into a DC output. A schematic for the AC/DC rectifier equivalent circuit diagram is illustrated in Fig. 8, which is an uncontrolled rectifier consisting of diodes in a bridge configuration. Since we need the maximum power from PZT, uncontrolled rectifier is preferred in this design.

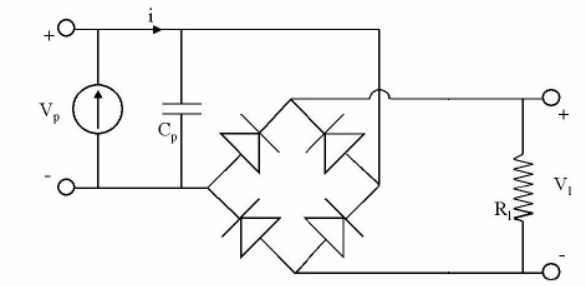

Fig. 8. Equivalent circuit for system with rectifier and load resistance.

Characterization of the power conversion circuits are conveyed with the PZT micropower generator device. Firstly, the power source is connected with a resistor bank that allows for setting different values of a resistor. After a resistance is set, the voltage at the resistor is measured. The voltage versus current characteristic is obtained when the measure points are connected. The power is given by a product of the voltage and current.

Fig. 9 shows the I-V characteristics of the PZT micropower generator with the rectifier circuit and load resistances. The experimental maximum voltage was ~7 V, the maximum power was ~140 μW. This matches the state-space model well, where the maximum voltage was ~9 V (peak), and the maximum power was ~145 μW.

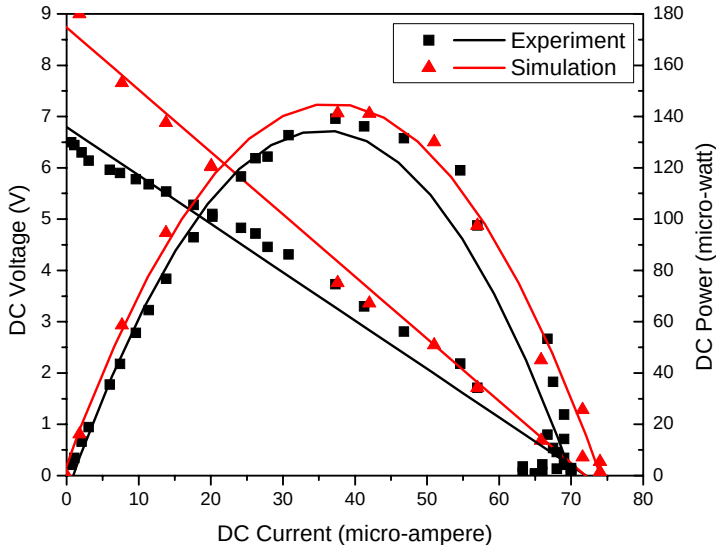

Fig. 9. Comparison of experimental vs. simulation DC I-V characteristics.

4.4. Rectifier with Resistive Load and 22 µF Capacitor

The PZT bender produces an alternating current, whose amplitude varies according to the amplitude of the acceleration and the frequency of vibration. On the other hand, electronic loads connected at the output require a DC voltage with relatively low amplitude. The AC/DC rectifier in the first stage converts the varying AC output voltage delivered by the PZT bender into a DC output. A schematic for the AC/DC rectifier with a 22 µF capacitor is illustrated in Fig. 10, which is an uncontrolled rectifier consisting of diodes in a bridge configuration. Since we need the maximum power from PZT, uncontrolled rectifier is preferred in this design.

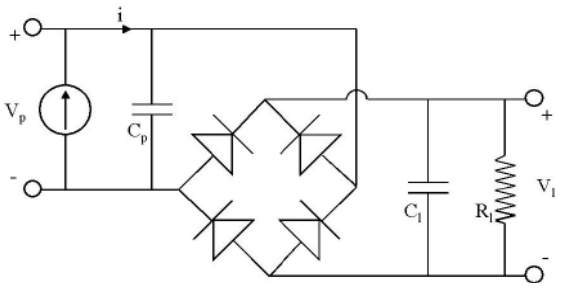

Fig. 10. Equivalent circuit for system with rectifier, capacitor and load resistance.

Fig. 11 shows the I-V characteristics of the PZT micropower generator with the rectifier circuit, 22 µf capacitor and load resistances. The experimental maximum voltage was ~9 V, the maximum power was ~120 µW. This however doesn't match very well with the state-space model well, where the maximum voltage was ~7 V (peak), and the maximum power was ~120 µW.

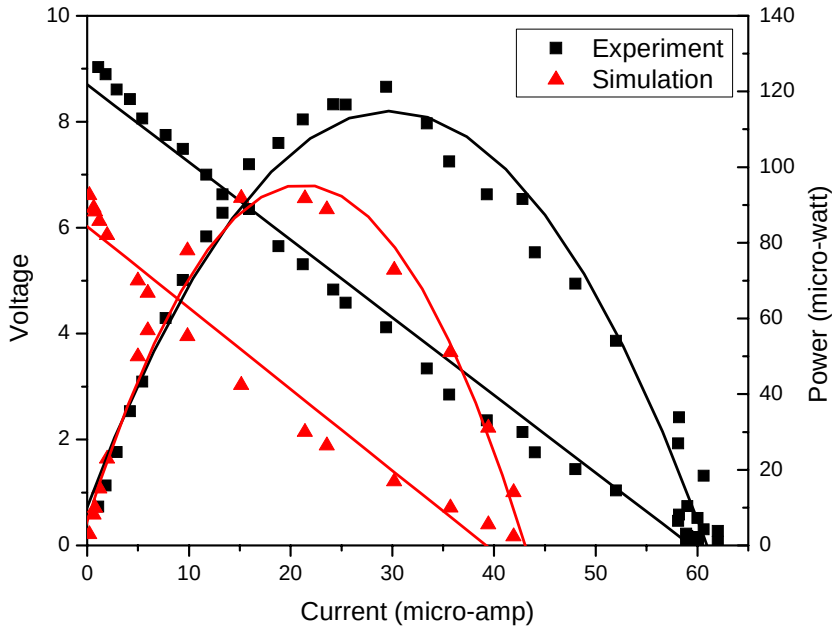

Fig. 11. Comparison of experimental vs. simulation DC I-V characteristics.

5. Conclusion and Discussion

Recent advancement in wireless and MEMS technology makes it possible to install sensors in remote locations and operate at very low power. The power sources currently chosen are based on batteries which demerits maintenance and prohibits integration inside of structures where sensors should permanently reside in. One potential solution is the use of PZT materials which can convert the ambient vibration energy surrounding them into electrical energy. The electrical energy can power other electronics devices or be stored for later use.

We have developed a model to predict the efficiency of power conversion for bimorph PZT cantilever beam based micropower generator. The derivation of the model has been provided, allowing it to be applied to a beam with various boundary conditions. The model was verified using experimental results and predicted the maximum power output quite well. Comparison of the model with the experiments revealed that the model can represent the output voltage waveform accurately.

Ultimately, the model developed provides a design tool for developing power harvesting systems by assisting in determining the size and extent of vibration needed to produce the desired level of power generation for both sinusoidal and noise inputs. The potential benefits of power harvesting and the advances in low power electronics and wireless sensors are making the future of this technology look very bright.

Discrepancies between the experimental results and the model are likely due to the following factors:
1) Uncertainties in the geometry of the device
2) Parasitic impedance in the actual device/sensing system
3) Unknown damping coefficient
4) Nonlinear piezoelectric properties

Using a root-sum-square uncertainty propagation method, it was found that a 5% uncertainty in the dimensions of the device causes an 11% uncertainty in the natural frequency of the device (2^{nd} order mechanical model). This alone could account in the discrepancy between the peak power frequencies. Another source of uncertainty is the elastic modulus of the PZT layers. The elastic modulus of PZT is dependent on the electrical boundary conditions. For the model, it was assumed the elastic modulus given was under open circuit conditions. To compensate, the value was multiplied by $(1-k^2)$ to get the approximate short circuit elastic modulus. This helped with matching the frequencies, but is still a source of uncertainty. Measuring the output might also affect the results; any parasitic impedance could affect the circuit, effecting the frequency and load at peak power. The damping coefficient is also very critical to the model, with lower damping causing the system poles to move towards the imaginary axis of the pole-zero map, however, this seems to effect the voltage and power outputs more than the frequency and load at max power. Lastly, the model uses linear piezoelectric properties. Because PZT properties often exhibit nonlinear and hysteretic behavior, the assumption of linear properties should be questioned.

The voltage and power results show that the model is fairly close to the experimental data when the natural frequencies match. The slight discrepancies present when natural frequency, output voltage and power are expected.

The flexibility in tailoring structure parameter can adjust generator property such as natural frequency, which increases potential of its application in various conditions. And the further work will be carried out to enhance the performance of the generator, which includes PZT MEMS devices and introduction of cantilevers array. Furthermore, efficient power conversion circuitry and management units should also be accomplished. Compared to reported micro-generators for vibration energy harvesting, our

device offers the advantage of good performance as far as promising voltage/power output and low natural frequency (to match general vibration sources) are concerned.

References

[1]. Roundy S., On the effectiveness of vibration-base energy harvesting, *Journal of Intelligent Material Systems and Structures,* 16, 2005, pp. 809-23.

[2]. Umeda M., Nakamura K. and Ueha S., Analysis of the transformation of mechanical impact energy to electric energy using piezoelectric vibrator, *Japanese Journal of Applied Physics,* 35, 1996, pp. 3267-3273.

[3]. Hausler E. and Stein E., Implantable physiological power supply with PVDF film, *Ferroelectronics,* 60, 1984, pp. 277–82.

[4]. Schmidt V. H., Piezoelectric energy conversion in windmills, *Proc. of IEEE Ultrasonics Symposium,* 1992, pp. 897–904.

[5]. Kymisis J., Kendall C., Paradiso J. and Gershenfeld N., Parasitic power harvesting in shoes, *2nd IEEE Int. Conf. on Wearable Computing,* 1998, pp. 132–137.

[6]. Kasyap A., Lim J., Johnson D., Horowitz S., Nishida T., Ngo K., Sheplak M. and Cattafesta L., Energy reclamation from a vibrating piezoelectric composite beam, *9th Annual Conf. on Sound and Vibration (Orlando, FL),* 2002, pp. 36–43.

[7]. Ramsay M. J. and Clark W. W., Piezoelectric energy harvesting for bio-MEMS application, *Smart Structures and Materials : Industrial and Commercial Applications of Smart Structures Technologies,* 4332, 2001, pp. 429-438.

[8]. Gonzalez J. L., Rubio A. and Moll F., Human powered piezoelectric batteries to supply power to wearable electronic devices, *International Journal- Society of Materials Engineering for Resources,* 10, Part 1, 2001, pp. 34-40.

[9]. Smits J. G. and Choi W. S., The constituent equations of piezoelectric heterogeneous bimorphs, *IEEE Transactions on Ultrasonics, Ferroelectrics, and Frequency Control,* 1991, 38.

[10]. Huang C., Lin Y. Y. and Tang T. A., Study on the tip-deflection of a piezoelectric bimorph cantilever in the static state, *Journal of Micromechanics and Microengineering,* 14, 2004, pp. 530-534.

[11]. DeVoe D. L. and Pisano A. P., Modeling and optimal design of piezoelectric cantilever microactuators, *Journal of Microelectromechanical Systems,* 6, No. 3, 1997, pp. 266-270.

[12]. Hwang W. S. and Park H. C., Finite element modeling of piezoelectric sensors and actuators, *AIAA Journal,* 31, No. 5, 1993, pp. 930-37.

[13]. Roundy S. and Wright P. K., A piezoelectric vibration based generator for wireless electronics, *Smart Materials and Structures,* 13, 2004, pp. 1131-1142.

[14]. Roundy S., Leland E. S., Baker J., Carleton E., Reilly E., Lai E., Otis B., Rabaey J. M., Wright P. K. and Sundararajan V., Improving power output for vibration-based energy scavengers, *IEEE Transactions on Pervasive Computing,* 4, Issue 1, 2005, pp. 28- 36.

[15]. Lu F., Lee H. P. and Lim S. P., Modeling and analysis of micro piezoelectric power generators for micro-electromechanical-systems applications, *Smart Materials and Structures,* 13, 2004, pp. 57-63.

[16]. Eggborn T., 2003, Analytical models to predict power harvesting with piezoelectric materials, *Mater's Thesis,* Virginia Polytechnic Institute and State University.

[17]. Kim S., 2002, Low power energy harvesting with piezoelectric generators, *PhD Thesis,* University of Pittsburgh.

[18]. Shen D., Ajitsaria J., Choe S. Y. and Kim D. J., The optimal design and analysis of piezoelectric cantilever beams for power generation devices, *Materials Research Society Symposium Proceedings,* 2006, p. 888.

[19]. Shu Y. C. and Lien I. C., Analysis of power output for piezoelectric energy harvesting systems, *Smart Materials and Structures,* 15, 2006, pp. 1499–1512.

[20]. Weinberg M., Working equations for piezoelectric actuators and sensors, *Journal of Microelectromechanical Systems,* 8, No. 4, 1999, pp. 529-33.
